ELSEVIER

Coordination Chemistry Reviews
174 (1998) 109–131

COORDINATION CHEMISTRY REVIEWS

A complete series of stepwise oxidation of $[Co(2\text{-pyridinethiolato})(en)_2]^{2+}$. Characterization of the 2-pyridinesulfenato-*N*,*S* and -*N*,*O*, 2-pyridinesulfinato-*N*,*S* and -*N*,*O*, and 2-pyridinesulfonato-*N*,*O* complexes

Mayumi Murata [a], Masaaki Kojima [a,*], Ayako Hioki [a], Miho Miyagawa [a], Masakazu Hirotsu [a], Kiyohiko Nakajima [b], Masakazu Kita [c], Setsuo Kashino [a], Yuzo Yoshikawa [a]

[a] *Department of Chemistry, Faculty of Science, Okayama University, Tsushima, Okayama 700-8530, Japan*
[b] *Department of Chemistry, Aichi University of Education, Igaya, Kariya 448-8542, Japan*
[c] *Department of Chemistry, Naruto University of Education, Takashima, Naruto 772-8502, Japan*

Received 31 July 1997; accepted 6 October 1997

Contents

Abstract

The H_2O_2 oxidation of $[Co(pyt)(en)_2]^{2+}$ [**1**, pyt = 2-pyridinethiolate(1−) ion, en = ethylenediamine] afforded the orange $[Co(pyse\text{-}N,S)(en)_2]^{2+}$ [**2**, pyse = 2-pyridinesulfenate(1−) ion]

* Corresponding author. Tel: +81 86 251 7842; Fax: +81 86 251 7842;
e-mail: kojima@cc.okayama-u.ac.jp

PII S0010-8545(97)00084-2

complex. Irradiation of this orange complex in the solid state yielded a green complex. The molecular structure of the green complex perchlorate was determined by X-ray diffraction to be $[Co(pyse\text{-}N,O)(en)_2](ClO_4)_2$ (**4**); linkage isomerization took place upon photolysis. The crystal data and final R value are: triclinic, $P\bar{1}$, $a=9.374(4)$ Å, $b=11.248(4)$ Å, $c=9.238(8)$ Å, $\alpha=95.26(4)^\circ$, $\beta=95.14(5)^\circ$, $\gamma=75.75(3)^\circ$, $V=938(2)$ Å^3, $Z=2$ and $R=0.040$ for 2757 unique reflections. The pyse-N,O complex has an anomalous feature in the UV–vis spectrum. It has an extra band ($16\,400\ cm^{-1}$) on the low-energy side of the first d–d absorption band ($22\,200\ cm^{-1}$). This band can be rationalized as a splitting component of the first d–d band generated by the anisotropic interaction of the antibonding π* orbital of the coordinating oxygen with the t_{2g} orbitals on the cobalt center. Treatment of $[Co(pyt)(en)_2]^{2+}$ with excess H_2O_2 afforded the yellow-orange sulfinato-N,S complex, $[Co(pysi\text{-}N,S)(en)_2]^{2+}$ [**3**, pysi = 2-pyridinesulfinate(1−) ion]. The molecular structure of the pysi-N,S complex was determined by X-ray diffraction to be $[Co(pysi\text{-}N,S)(en)_2](ClO_4)_2$ (**3**), which cocrystallized with the pysi-N,O complex (**5**). The crystal data and final R value for the cocrystal (**3/5**) are: monoclinic, $C2$, $a=28.559(8)$ Å, $b=6.960(2)$ Å, $c=10.406(3)$ Å, $\beta=99.90\ (2)^\circ$, $V=2038(2)$ Å^3, $Z=4$ and $R=0.040$ for 2391 unique reflections. The pysi-N,S complex was unstable and was easily converted photochemically or thermally to the linkage-isomerized orange pysi-N,O complex (**5**). The sulfur atom becomes chiral (R and S) upon linkage isomerization, and two kinds of racemic salt, $\Lambda(R)\Delta(S)$ and $\Lambda(S)\Delta(R)$, were separated by fractional crystallization of the complex perchlorate. The molecular structure of the less soluble isomer ($\Lambda(S)\Delta(R)$-**5**) of the perchlorate was determined by X-ray diffraction to be $\Lambda(S)\Delta(R)$-$[Co(pysi\text{-}N,O)(en)_2](ClO_4)_2$. The crystal data and final R value are: triclinic, $P\bar{1}$, $a=9.384(4)$ Å, $b=11.807(8)$ Å, $c=8.640(5)$ Å, $\alpha=98.54(5)^\circ$, $\beta=94.40(4)^\circ$, $\gamma=96.65(5)^\circ$, $V=936(2)$ Å^3, $Z=2$ and $R=0.038$ for 3061 unique reflections. The two diastereomers of Λ-$[Co(pysi\text{-}N,O)(en)_2]^{2+}$ were separated by SP-Sephadex column chromatography, and one of them ($\Lambda(R)$-**5**) was structurally characterized by X-ray crystallography. $\Lambda(R)$-$[Co(pysi\text{-}N,O)(en)_2](ClO_4)_2$, which crystallizes as orthorhombic in space group $P2_12_12_1$ with $Z=4$, has the cell parameters $a=9.896(2)$ Å, $b=20.758(6)$ Å, $c=9.494(4)$ Å, $V=1950(2)$ Å^3. The final R value was 0.041 for 1543 unique reflections. Kinetic studies of reversible isomerization (epimerization) between $\Lambda(R)$- and $\Lambda(S)$-$[Co(pysi\text{-}N,O)(en)_2]^{2+}$ were performed in aqueous solutions at 60 °C. The rate constants were $k_{\Lambda(R)\rightarrow\Lambda(S)}=5.5\times10^{-6}\ s^{-1}$ and $k_{\Lambda(S)\rightarrow\Lambda(R)}=1.7\times10^{-6}\ s^{-1}$. The orange-red $[Co(pyso\text{-}N,O)(en)_2]^{2+}$ [**6**, pyso = 2-pyridinesulfonate(1−) ion] complex was prepared by the reaction of *cis*-$[Co\{OS(O)_2CF_3\}_2(en)_2]^+$ with the 2-pyridinesulfonate ligand or by the oxidation of $[Co(pyse\text{-}N,O)(en)_2]^{2+}$ (**4**) with H_2O_2. The molecular structure of the trifluoromethanesulfonate salt of complex **6** was determined by X-ray diffraction. $[Co(pyso\text{-}N,O)(en)_2](CF_3SO_3)_2$ crystallizes as monoclinic in space group $P2_1/a$ with $Z=4$. The cell parameters are $a=19.079(8)$ Å, $b=16.699(6)$ Å, $c=7.462(4)$ Å, $\beta=100.51(4)^\circ$, $V=2338(2)$ Å^3. The final R value was 0.050 for 3966 unique reflections. The pyso ligand has the strongest ligand field strength among the ligands studied here. A series of sulfur oxidation from $[Co(pyt)(en)_2]^{2+}$ to $[Co(pyso\text{-}N,O)(en)_2]^{2+}$ is established.

Keywords: Ligand oxidation; Cobalt complexes; Thiolato complexes; Sulfenato complexes; Sulfinato complexes; Sulfonato complexes

1. Introduction

Many cobalt(III) complexes containing five-membered thiolate chelates such as 2-aminoethanethiolate have been prepared and their oxidation reactions have been

studied extensively [1–5]. Stoichiometric oxidation of a thiolato complex gives the corresponding sulfenato-*S* complex, and subsequent oxidation converts the sulfenato-*S* complex to the sulfinato-*S* complex.

2-Pyridinethiolate(1−) (=pyt) is an aromatic ligand and forms a four-membered didentate-*N*,*S* chelate upon coordination. In the previous paper [4], we reported that the stereochemistry and the oxidation reactivity of pyt–cobalt(III) complexes such as $[Co(pyt)(en)_2]^{2+}$ (**1**), are quite different from those of the 2-aminoethanethiolate–cobalt(III) ones. For example, the orange 2-pyridinesulfenato (=pyse) complex, which is the oxidation product of **1**, was photochemically converted to a green complex in the solid state. Such a reaction has never been observed in the corresponding 2-aminoethanethiolato or other related complexes. The orange and green complexes were assigned to $[Co(pyse\text{-}N,S)(en)_2]^{2+}$ (**2**) and $[Co(pyse\text{-}N,O)(en)_2]^{2+}$ (**4**), respectively, on the basis of their UV–vis and X-ray photoelectron spectra. Here, we report the X-ray structure analysis of the green complex **4**. We studied the subsequent oxidation, and obtained $[Co(pysi\text{-}N,S)(en)_2]^{2+}$ [**3**, pysi=2-pyridinesulfinate(1−) ion], $[Co(pysi\text{-}N,O)(en)_2]^{2+}$ (**5**) and $[Co(pyso\text{-}N,O)(en)_2]^{2+}$ [**6**, pyso=2-pyridinesulfonate(1−) ion]. Thus, a series of sulfur oxidation from **1** to **6** is established (Scheme 1). This paper also describes the characterization, reactivity and X-ray structure analyses of **3**, **5** and **6**.

2. Experimental

2.1. Materials

2-Pyridinesulfonic acid was prepared by oxidizing 2-mercaptopyridine with nitric acid [6]. Sodium 2-pyridinesulfonate was obtained by neutralizing the acid with sodium carbonate [7].

Caution! Perchlorate salts of metal complexes can be explosive and should be handled with care.

2.1.1. Preparation of $[Co(pyse\text{-}N,O)(en)_2](ClO_4)_2$ (**4**)

The orange $[Co(pyse\text{-}N,S)(en)_2](ClO_4)_2$ complex (**2**) [4], which was prepared by oxidizing **1**, was irradiated in the solid state with a high-pressure mercury lamp through a Pyrex glass filter, which allows only visible light to pass through, to afford a green complex. The green complex was purified by SP-Sephadex column chromatography. On elution with 0.3 M (1 M=1 mol dm^{-3}) $NaClO_4$, the column showed two bands, orange (small amount, unreacted **2**) and green in the order of elution. From the eluate containing the green band, the perchlorate salt of complex **4** was obtained. Anal. Found: C, 21.03; H, 3.84; N, 13.44%. Calcd for $C_9H_{20}N_5Cl_2CoO_9S$: C, 21.44; H, 4.00; N, 13.89%. The optically active **4** was prepared in the same manner starting from the optically active **1** [4]. The optically active **4** could not be isolated, because it racemizes during crystallization. Thus, the eluate containing the green band was used for the CD spectrum measurement, and the

concentration of the solution was estimated on the basis of the absorbance at 607 nm. One of the crystals which racemized during crystallization was used for X-ray structure analysis.

2.1.2. Preparation of [Co(pysi-N,S)(en)$_2$](ClO$_4$)$_2$ (**3**) and [Co(pysi-N,O)(en)$_2$](ClO$_4$)$_2$ (**5**)

All procedures were carried out in the dark. A mixture of 30% H_2O_2 (2 g, 18 mmol) and 60% $HClO_4$ (2 g) was added dropwise to a DMSO (dimethyl sulfoxide) solution (5 cm^3) of Λ-[Co(pyt)(en)$_2$](ClO$_4$)$_2$ (**1**, 0.5 g, 1 mmol) with stirring below 5 °C. The color of the solution changed from brown to yellow-orange during the addition. The mixture was stirred for 30 min and left overnight in a refrigerator. Addition of diethyl ether (1400 cm^3) and ethanol (600 cm^3) to the resulting solution and cooling in an ice bath gave a yellow-orange precipitate. It was recrystallized from water. Anal. Found: C, 21.12; H, 4.07; N, 12.89; S, 6.30%. Calcd for $C_9H_{20}CoCl_2N_5O_{10}S$ = Λ-[Co(pysi-*N*,*S*)(en)$_2$](ClO$_4$)$_2$ (**3**): C, 20.78; H, 3.88; N, 13.46; S, 6.16%. Suitable crystals (**3/5**) for X-ray analysis were obtained by slow evaporation of an aqueous solution at room temperature. The X-ray crystal structure analysis revealed that **3** cocrystallized with **5** (*vide infra*).

The yellow-orange reaction mixture was diluted with water (200 cm^3) and exposed to sunlight for a day to induce linkage isomerization. The reaction was accompanied by a color change from yellow-orange to orange. The orange solution was charged on top of an SP-Sephadex C-25 column (145 cm × 3 cm ID). Upon elution with 0.15 M $Na_2[Sb_2\{(+)\text{-tart}\}_2]$, there was an indication of separation, and the initial and final fractions were collected separately. Each was diluted with a large amount of water and poured again onto a small SP-Sephadex C-25 column (2 cm × 3 cm ID). The adsorbed complex was eluted with 0.5 M $NaClO_4$. The eluate was evaporated to ca. 5 cm^3 under reduced pressure to yield an orange precipitate. It was recrystallized from water. The faster eluted isomer was determined to have the Λ(*R*) configuration from X-ray analysis. For elemental analysis, the Δ isomers (Δ(*R*) and Δ(*S*)) were used. The Δ diastereomers were prepared in the same manner. For separation of the Δ diastereomers, 0.3 M NaCl was used as the eluent. The CD spectrum of the faster eluted isomer indicated that the complex has the Δ(*R*) configuration. Anal. Found for the faster eluted isomer, Δ(*R*): C, 20.66; H, 4.04; N, 13.10; S, 6.23%. Found for the slower eluted isomer, Δ(*S*): C, 21.00; H, 4.13; N, 13.19; S, 6.46%. Calcd for $C_9H_{20}CoCl_2N_5O_{10}S$ = [Co(pysi-*N*,*O*)(en)$_2$](ClO$_4$)$_2$: C, 20.78; H, 3.88; N, 13.46; S, 6.16%. Starting with racemic **1**, we obtained racemic **5**. It was recrystallized from water several times, and the Λ(*S*)Δ(*R*)-isomer was obtained as the less soluble salt. This salt was also used for the X-ray structure determination.

2.1.3. Preparation of [Co(pyso-N,O)(en)$_2$]X$_2$ (**6**, X = CF$_3$SO$_3$, ClO$_4$)

This complex was prepared in two ways, (i) and (ii):

(i) To a suspension of *cis*-$[Co\{OS(O)_2CF_3\}_2(en)_2]CF_3SO_3$ [8] (0.64 g, 1 mmol) in methanol (15 cm^3) was added a methanol solution (15 cm^3) of sodium 2-pyridinesulfonate [7] (0.18 g, 1 mmol). The mixture was refluxed for 15 min to give an orange solution and then evaporated to ca. 5 cm^3. Orange-red crystals, which

deposited upon cooling, were collected by filtration and washed with a small amount of methanol. Yield: 0.40 g. Anal. Found: C, 20.93; H, 2.87; N, 10.95; S, 15.18%. Calcd for $C_{11}H_{20}N_5CoF_6O_9S_3$ = [Co(pyso-*N*,*O*)(en)$_2$](CF$_3$SO$_3$)$_2$: C, 20.79; H, 3.17; N, 11.02; S, 15.14%. One of the crystals (**6**) was used for X-ray structure analysis. This pyso complex was resolved by SP-Sephadex C-25 column chromatography, 0.1 M $Na_2[Sb_2\{(+)\text{-tart}\}_2]$ being used as the eluent. The column showed two bands, Λ and Δ, in the order of elution. Each eluate was diluted with water and passed through a small column of SP-Sephadex C-25. The adsorbed complex was eluted with 1 M $NaClO_4$, and the eluate was used for measurements.

(ii) A mixture of 30% H_2O_2 (5 g, 45 mmol) and 60% $HClO_4$ (5 g) was added dropwise to a DMSO solution (7.5 cm^3) of [Co(pyse-*N*,*O*)(en)$_2$](ClO$_4$)$_2$ (**4**, 0.53 g, 1 mmol) with stirring below 5 °C. The color of the solution changed from green to orange during the addition. The mixture was stirred for 30 min and left overnight in a refrigerator. The orange reaction mixture was diluted with water (500 cm^3) and was charged on top of an SP-Sephadex C-25 column (90 cm × 3 cm ID). Upon elution with 0.15 M Na_2SO_4, two orange bands were developed. The UV–vis spectrum of the faster eluted complex indicated the formation of $[Co(pyso\text{-}N,O)(en)_2]^{2+}$. The slower eluted complex was assigned to $[Co(pysi\text{-}N,O)(en)_2]^{2+}$ on the basis of the UV–vis spectrum. The eluate containing the sulfonato complex was evaporated to ca. 5 cm^3 under reduced pressure. To the concentrate a saturated aqueous $NaClO_4$ (3 g) solution was added. The mixture was slowly evaporated under reduced pressure to yield orange-red crystals, which were collected, washed successively with cold water and methanol, and then dried in a desiccator over P_4O_{10}. Anal. Found: C, 20.30; H, 4.09; N,13.04; S, 6.11%. Calcd for $C_9H_{20}N_5Cl_2CoO_{11}S$ = [Co(pyso-*N*,*O*)(en)$_2$](ClO$_4$)$_2$: C, 20.16; H, 3.76; N, 13.04; S, 5.98%.

2.2. Instruments used

UV–vis and circular dichroism (CD) spectra were recorded on JASCO Ubest-30, Ubest V-550 and UVIDEC-610 spectrophotometers, and a JASCO J-720 spectropolarimeter, respectively. ^{1}H NMR spectra were measured in D_2O with TSP [sodium 3-(trimethylsilyl)propionate-2,2,3,3-d_4] as an internal reference, and recorded on a Varian VXR-500 spectrometer. Elemental analyses were carried out on a Perkin Elmer 2400 II organic elemental analyzer.

2.3. Thermal kinetics

The rate of linkage isomerization from Λ-$[Co(pysi\text{-}N,S)(en)_2]^{2+}$ to Λ-$[Co(pysi\text{-}N,O)(en)_2]^{2+}$ was studied in water by following the CD change in the 350–600 nm range at 30 °C. Throughout the reaction an isodichroic point was observed at 513 nm.

Kinetic studies of reversible isomerization (epimerization) between Λ(*R*)-$[Co(pysi\text{-}N,O)(en)_2]^{2+}$ and Λ(*S*)-$[Co(pysi\text{-}N,O)(en)_2]^{2+}$ were performed in aqueous solutions by following the CD strengths change at 325 nm at 60 °C.

2.4. Electrochemical measurements

All complexes (**4**, **5** and **6**) showed irreversible redox behavior in CV (cyclic voltammetry), and the reduction potentials were obtained by RDE (rotating-disk electrode) measurements. RDE measurements were carried out in aqueous solutions (complex concentration: 1.0×10^{-3} M in 0.1 M KCl) at room temperature using a FUSO HECS 321B potential sweep unit and a FUSO HECS 312B potentiostat. A glassy-carbon rotating-disk (2000 rpm) attached to a Yanako P10-RE Mark II head, a platinum wire and SCE were used as the working, auxiliary and reference electrodes, respectively. The oxidation wave of $K_4[Fe(CN)_6]$ was observed at $+0.275$ V vs SCE under these conditions.

2.5. X-ray structure determination

Single crystals of the perchlorate salts of complexes **3/5**, **4**, $\Lambda(S)\Delta(R)$-**5**, $\Lambda(R)$-**5** and the trifluoromethanesulfonate salt of complex **6**, were obtained as described above. Each crystal was mounted on a glass fiber. The diffraction data were collected using a Rigaku AFC-5R diffractometer with graphite monochromatized Mo Kα radiation ($\lambda = 0.71073$ Å) at the X-Ray Laboratory of Okayama University except for **6**, for which the data were obtained at the Institute for Molecular Science. Lattice parameters were determined with 25 reflections in the 2θ range 21–22° for **3/5**, 22–23° for **4**, 22–23° for $\Lambda(S)\Delta(R)$-**5**, 21–22° for $\Lambda(R)$-**5** and 24–25° for **6**. The intensities of three standard reflections were monitored after every 97 reflections; in all cases no significant variations were observed. The intensities were corrected for Lorentz and polarization effects, and empirical absorption correction was applied. The structures were solved by a direct method [9] and refined anisotropically for non-H atoms by a full-matrix least-squares procedure except for **3/5**. The structure for **3/5** was refined by a block diagonal matrix procedure, and the positions of several hydrogen atoms were identified in a subsequent difference Fourier map, but the others were fixed at calculated positions and only their isotropic displacement parameters were refined. In the structure of **3/5**, the chlorine atoms of ClO_4 ions appeared at a general position and special positions *b*2 and *a*2. One oxygen atom of the ClO_4 ion occupying each special position was found on the 2-fold axis, and the other oxygen atoms were disordered around the 2-fold axis. Further, a difference Fourier map showed a disorder at the sulfinate site of the chelate ring. The disordered structure was successfully refined by assuming a static disorder of the sulfinate moiety between the *S*-bonded complex (**3**) and the *O*-bonded one (**5**). The occupancy factor was determined to be 0.675 for **3** and 0.325 for **5**. Although the oxygen atom, O(2)′ [primed atoms denote the disordered moiety (**5**) in **3/5**] may be disordered with respect to sulfur chirality (*R* and *S*, *vide infra*), no additional peak was found. For **4**, all hydrogen atoms were fixed at ideal positions with isotropic displacement parameters of 1.2 times those of the nitrogen and carbon atoms to which the H atoms are attached. For $\Lambda(S)\Delta(R)$-**5** and $\Lambda(R)$-**5**, the positions of several hydrogen atoms were identified in subsequent difference Fourier maps. For **6**, all hydrogen atoms were placed at calculated positions and the isotropic displacement parameters

Table 1
Crystallographic data and experimental details

	4	**3/5**	Λ(*S*)Δ(*R*)-**5**	Λ(*R*)-**5**	**6**
Formula	$C_9H_{20}N_5Cl_2CoO_9S$	$C_9H_{22}N_5Cl_2CoO_{11}S$	$C_9H_{20}N_5Cl_2CoO_{10}S$	$C_9H_{20}N_5Cl_2CoO_{10}S$	$C_{11}H_{20}N_5CoF_6O_9S_3$
FW	504.18	538.20	520.18	520.18	635.43
Crystal system	Triclinic	Monoclinic	Triclinic	Orthorhombic	Monoclinic
Space group	$P\bar{1}$	$C2$	$P\bar{1}$	$P2_12_12_1$	$P2_1/a$
a (Å)	9.374(4)	28.559(8)	9.384(4)	9.896(2)	19.079(8)
b (Å)	11.248(4)	6.960(2)	11.807(8)	20.758(6)	16.699(6)
c (Å)	9.238(8)	10.406(3)	8.640(5)	9.494(4)	7.462(4)
α (deg)	95.26(4)		98.54(5)		
β (deg)	95.14(5)	99.90(2)	94.40(4)		100.51(4)
γ (deg)	75.75(3)		96.65(5)		
Z	2	4	2	4	4
V (Å^3)	938(2)	2038(2)	936(2)	1950(2)	2338(2)
μ(Mo Kα) (mm^{-1})	1.36	1.26	1.37	1.31	1.10
Crystal color	Green	Red	Orange	Red	Orange-red
Crystal habit	Prismatic	Prismatic	Prismatic	Prismatic	Prismatic
Crystal size (mm^3)	$0.33\times0.33\times0.43$	$0.45\times0.01\times0.68$	$0.33\times0.16\times0.45$	$0.17\times0.15\times0.25$	$0.30\times0.40\times0.40$
D_x (g cm^{-3})	1.785	1.754	1.845	1.771	1.806
$F(000)$	516	1104	532	1064	1288
T (K)	295	298	298	297	298
Scan range (deg)	$1.73+0.30\tan\theta$	$1.78+0.30\tan\theta$	$1.52+0.30\tan\theta$	$0.84+0.30\tan\theta$	$1.90+0.50\tan\theta$
Scan mode	$\omega-2\theta$	$\omega-2\theta$	$\omega-2\theta$	$\omega-2\theta$	ω
Scan speed (deg min^{-1})	6	6	6	4	8
$2\theta_{max}$ (deg)	55	55	55	52	60
Reflections measd	$-11\le h\le11$	$-37\le h\le37$	$-12\le h\le12$	$0\le h\le12$	$-26\le h\le26$
	$-13\le k\le13$	$0\le k\le9$	$-15\le k\le15$	$0\le k\le25$	$0\le k\le23$
	$0\le l\le10$	$-14\le l\le14$	$0\le l\le11$	$-1\le l\le11$	$0\le l\le9$
No. of reflections measd	4578	5039	4586	2492	6081
R_{int}	0.010	0.024	0.010	0.032	0.032
No. of reflections obsd	2757	2391	3061	1543	3966
	$I>3.0\sigma(I)$	$I>2.0\sigma(I)$	$I>3.0\sigma(I)$	$I>3.0\sigma(I)$	$F>3.0\sigma(F)$
No. of parameters refined	244	451	333	334	376
R[a]	0.040	0.040	0.038	0.041	0.050
R_w[b]	0.042	0.039	0.030	0.030	0.053
S	3.85	4.15	2.27	1.91	1.83
$(\Delta/\delta)_{max}$	0.02	0.27	0.03	0.53	0.32
Largest diff peak (e Å^{-3})	0.66	0.47	0.70	0.38	0.38
Largest diff hole (e Å^{-3})	−0.53	−0.40	−0.56	−0.42	−0.81

[a] $R=\Sigma\,||F_o|-|F_c||/\Sigma\,|F_o|$.

[b] $R_w=[\Sigma\,w(|F_o|-|F_c|)^2/\Sigma\,w|F_o|^2]^{1/2}$, $w=1/\sigma^2(F_o)$.

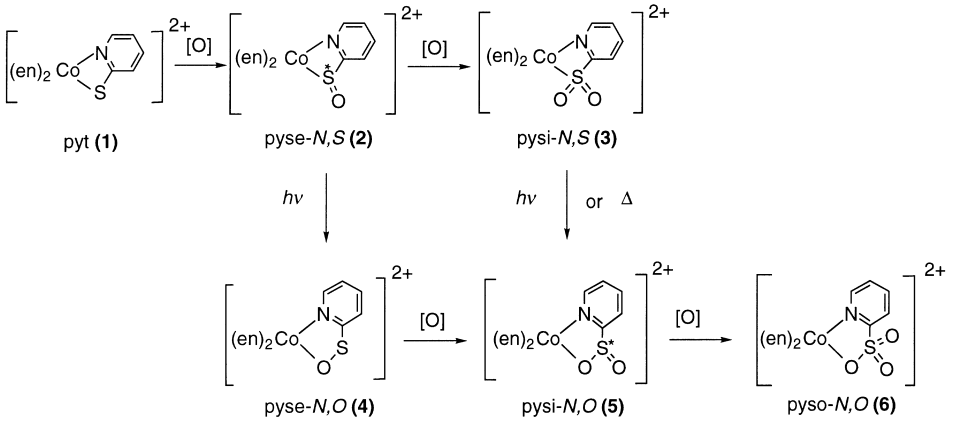

Scheme 1. Oxidation and isomerization of the complexes.

were fixed to be equal to those of the parent nitrogen and carbon atoms. The calculations were performed using TEXSAN [10] except for **6**, for which the calculations were performed using Xtal 3.2 [11]. Crystal data and experimental details are listed in Table 1. Crystallographic data (excluding structure factors) for the structures reported in this paper have been deposited with the Cambridge Crystallographic Data Centre, 12 Union Road, Cambridge CB2 1EZ, England, as supplementary publication No. 101275.

2.6. Theoretical calculations

The optimal geometries of the *O*-bonded complexes **4**, **5** and **6** were determined by RHF calculations using the ZINDO program with INDO/1 parameters [12]. The

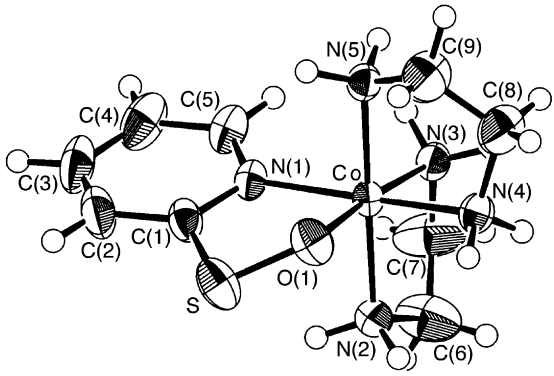

Fig. 1. An ORTEP drawing for the complex cation, $[Co(pyse\text{-}N,O)(en)_2]^{2+}$ (**4**), with thermal ellipsoids at 50% probability.

Table 2
Selected bond lengths [l (Å)] and bond angles [φ (deg)] for $[Co(pyse\text{-}N,O)(en)_2]^{2+}$ (**4**)

Co–O(1)	1.893(3)	Co–N(1)	1.963(3)
Co–N(2)	1.968(3)	Co–N(3)	1.977(3)
Co–N(4)	1.958(3)	Co–N(5)	1.943(3)
S–O(1)	1.581(3)	S–C(1)	1.733(5)
N(1)–C(1)	1.356(5)	N(1)–C(5)	1.339(5)
N(2)–C(6)	1.473(6)	N(3)–C(7)	1.479(6)
N(4)–C(8)	1.471(5)	N(5)–C(9)	1.458(5)
C(1)–C(2)	1.383(6)	C(2)–C(3)	1.361(7)
C(3)–C(4)	1.380(7)	C(4)–C(5)	1.373(6)
C(6)–C(7)	1.389(7)	C(8)–C(9)	1.424(7)
O(1)–Co–N(1)	87.1(1)	O(1)–Co–N(2)	91.8(1)
O(1)–Co–N(3)	175.4(1)	O(1)–Co–N(4)	85.2(1)
O(1)–Co–N(5)	88.0(1)	N(1)–Co–N(2)	91.4(1)
N(1)–Co–N(3)	96.2(1)	N(1)–Co–N(4)	170.9(1)
N(1)–Co–N(5)	89.3(1)	N(2)–Co–N(3)	85.0(1)
N(2)–Co–N(4)	93.6(1)	N(2)–Co–N(5)	179.2(1)
N(3)–Co–N(4)	91.8(1)	N(3)–Co–N(5)	95.1(1)
N(4)–Co–N(5)	85.7(1)	Co–O(1)–S	114.3(2)
Co–N(1)–C(1)	114.3(3)	Co–N(1)–C(5)	127.5(3)
Co–N(2)–C(6)	110.6(3)	Co–N(3)–C(7)	108.8(3)
Co–N(4)–C(8)	109.6(3)	Co–N(5)–C(9)	109.6(3)
O(1)–S–C(1)	99.9(2)	S–C(1)–N(1)	115.7(3)
S–C(1)–C(2)	122.5(4)	C(1)–N(1)–C(5)	118.0(3)
C(1)–C(2)–C(3)	119.3(4)	C(2)–C(3)–C(4)	119.2(4)
C(3)–C(4)–C(5)	119.2(4)	N(1)–C(1)–C(2)	121.8(4)
N(1)–C(5)–C(4)	122.3(4)	N(2)–C(6)–C(7)	112.1(4)
N(3)–C(7)–C(6)	113.1(4)	N(4)–C(8)–C(9)	111.2(4)
N(5)–C(9)–C(8)	111.2(4)		

Mulliken bond orders of the ZINDO optimized structures were estimated by the extended Hückel method.

Strain-energy minimization calculations were carried out for complexes **2**, **3**, **4** and **5** with a modified MM2 computer program [13,14] in order to obtain their relative strain energy and to estimate the stable structure between the isomers. The initial atomic coordinates were obtained from crystallographic data, if these were available. For **2**, the same coordinates as those for **3** were used except that one of the oxygen atoms [O(1) for $\Lambda(S)$, O(2) for $\Lambda(R)$] was replaced with a lone-pair. For **5**, the coordinates of **6** were used and one of the oxygen atoms [O(2) for $\Lambda(S)$, O(3) for $\Lambda(R)$] was replaced with a lone-pair. To avoid local minima in the force field, two or more distinct initial atomic coordinates were used for calculations and they gave essentially the same results. The parameters for the present force fields were mainly adopted from those of MM2 (1985), MM2 and MMP2 (1986), and the literature [15]. The parameters used for the calculations for the four-membered complexes (**2** and **3**) were the same as for the five-membered ones (**4** and **5**). The electrostatic interactions were not considered for these calculations.

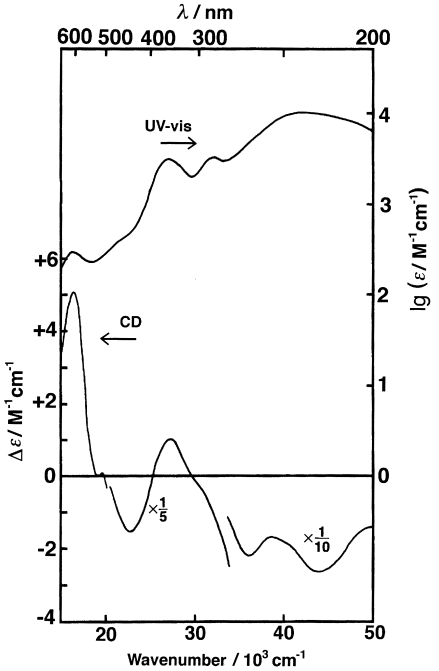

Fig. 2. UV–vis and CD spectra of Λ-[Co(pyse-*N*,*O*)(en)$_2$](ClO$_4$)$_2$ (Λ-**4**).

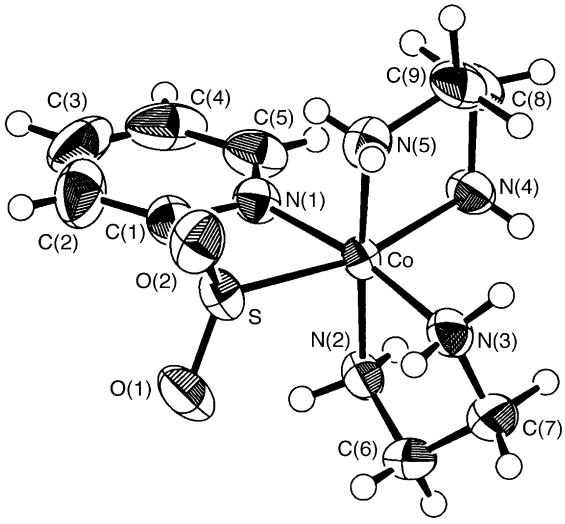

Fig. 3. An ORTEP drawing for the complex cation, [Co(pysi-*N*,*S*)(en)$_2$]$^{2+}$ (**3**), in cocrystal **3/5**. The sulfinate site of **5** is omitted for clarify. The thermal ellipsoids are drawn at 50% probability.

Table 3
UV–vis and CD spectral data in water

Complex	UV–vis Wavenumber$_{max}$/10^3 cm^{-1} (log ϵ/M^{-1} cm^{-1})	CD Wavenumber$_{ext}$/10^3 cm^{-1} ($\Delta\epsilon$/M^{-1} cm^{-1})
Λ-[Co(pyse-*N,O*)(en)$_2$]$^{2+}$ (Λ-**4**)	16.4 (2.49), 22.2 (2.64), 27.2 (3.51), 32.3 (3.52), 46.4 (4.42)	16.6 (+5.06), 19.8 (−0.13), 23.1 (−7.72), 27.6 (+5.11), 36.3 (−22.1), 44.0 (−26.5)
Λ-[Co(pysi-*N,S*)(en)$_2$]$^{2+}$ (Λ-**3**)	21.8 (2.33), 31.5 (3.71), 38.9 (sh, 3.83), 47.6 (4.37)	20.9 (+2.55), 26.6 (−0.40), 32.3 (−6.62), 44.0 (−23.2)
Λ(*R*)-[Co(pysi-*N,O*)(en)$_2$]$^{2+}$ (Λ(*R*)-**5**)	20.2 (1.91), 29.4 (3.03), 38.2 (sh, 3.82), 44.5 (sh, 4.28)	19.8 (+1.17), 24.4 (+0.19), 30.3 (−5.29), 35.4 (−2.68), 39.4 (−1.01), 44.5 (−19.7)
Λ(*S*)-[Co(pysi-*N,O*)(en)$_2$]$^{2+}$ (Λ(*S*)-**5**)	20.2 (1.97), 29.4(3.06), 38.2 (sh, 3.83), 43.9 (sh, 4.22)	18.8 (+3.66), 22.5 (+0.32), 24.9 (−0.037), 28.8 (+0.48), 31.9 (−0.77), 34.5 (−0.053), 39.0 (−8.57), 46.0 (−33.7)
Λ-[Co(pyso-*N,O*)(en)$_2$]$^{2+}$ (Λ-**6**)	20.6 (1.90), 29.0 (1.97), 37.5 (sh, 3.75), 47.6 (4.40)	18.6 (+2.58), 20.8 (−0.04), 22.5 (+0.40), 26.4 (+0.26), 29.8 (+0.50), 38.2 (−6.20), 45.4 (−52.9)

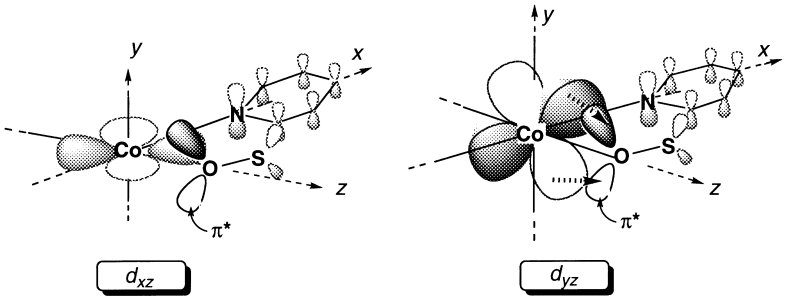

Scheme 2. Interaction of the π* orbital with the d_{xz} and d_{yz} orbitals in **4**.

3. Results and discussion

3.1. Sulfenato complex

In the previous paper [4], we reported that the oxidation of $[Co(pyt)(en)_2]^{2+}$ (**1**) gave an orange complex, and that the orange complex was photochemically converted into a green one in the solid state (Scheme 1). We assigned the orange and green complexes as $[Co(pyse\text{-}N,S)(en)_2]^{2+}$ (**2**) and $[Co(pyse\text{-}N,O)(en)_2]^{2+}$ (**4**), respectively, on the basis of the UV–vis and X-ray photoelectron spectra [4]. The X-ray analysis of the green complex supports these assignments.

Fig. 1 shows a perspective view of the green complex cation, $[Co(pyse\text{-}N,O)(en)_2]^{2+}$ (**4**). Bond lengths and angles are listed in Table 2. The coordination geometry around the cobalt atom is approximately octahedral. The pyse ligand coordinates to cobalt with the nitrogen and oxygen instead of the nitrogen and sulfur as in the parent orange complex, $[Co(pyse\text{-}N,S)(en)_2]^{2+}$ (**2**), and the number of chelate ring members increases from four to five. The sulfur–oxygen bond, S–O(1) (1.581(3) Å) is longer than that in the *S*-bonded $[Co\{S(O)CH_2CH_2NH_2\text{-}N,S\}(en)_2](SCN)_2$ complex (1.552(3) Å) [2]. The bond angle of O(1)–Co–N(1) (87.1(1)°) is larger than the S–Co–N (72.6(2)°) angle for the four-membered chelate ring in $[Co(pyt)(en)_2](ClO_4)_2$ [4]. The *O*-bonded sulfenate ligand exerts a small trans influence; the Co–N bond trans to the pyse sulfur is longer than the average of the *cis* Co–N bonds by 0.021(4) Å. This is in marked contrast to the large trans influence (0.072(8) Å) associated with the *S*-bonded sulfenate ligand in $[Co\{S(O)CH_2CH_2NH_2\text{-}N,S\}(en)_2](SCN)_2$ [2]. To our knowledge, the present study provides the first definitive evidence for the existence of a sulfenato-*O* cobalt(III) complex.

Although we have reported the UV–vis and CD spectra of $[Co(pyse\text{-}N,O)(en)_2]^{2+}$, the complex was contaminated with the *N*,*S*-complex as evidenced by the X-ray photoelectron spectrum [4]. We now present the spectra of the *N*,*O*-isomer (**4**) purified by SP-Sephadex column chromatography (Fig. 2 and Table 3). The first d–d absorption band of this complex might be the one at 22 200 cm^{-1}. This complex has an extra band (16 400 cm^{-1}) on the low-energy side of the first d–d absorption band. This band will be interpreted as a splitting compo-

Table 4
Selected bond lengths [l (/Å)] and bond angles [φ (deg)] for $[Co(pysi\text{-}N,S)(en)_2]^{2+}$ (**3**) determined from the cocrystal (**3/5**)

Co–S	2.179(2)	Co–N(1)	1.952(3)
Co–N(2)	1.975(4)	Co–N(3)	1.950(3)
Co–N(4)	1.988(4)	Co–N(5)	1.961(4)
S–O(1)	1.465(5)	S–O(2)	1.431(5)
S–C(1)	1.866(4)	N(1)–C(1)	1.358(7)
N(1)–C(5)	1.339(6)	N(2)–C(6)	1.482(5)
N(3)–C(7)	1.508(8)	N(4)–C(8)	1.496(6)
N(5)–C(9)	1.490(6)	C(1)–C(2)	1.356(7)
C(2)–C(3)	1.364(9)	C(3)–C(4)	1.38(1)
C(4)–C(5)	1.371(7)	C(6)–C(7)	1.498(7)
C(8)–C(9)	1.499(8)		
S–Co–N(1)	72.9(1)	S–Co–N(2)	94.9(1)
S–Co–N(3)	99.4(2)	S–Co–N(4)	165.2(1)
S–Co–N(5)	87.0(1)	N(1)–Co–N(2)	90.1(1)
N(1)–Co–N(3)	170.6(2)	N(1)–Co–N(4)	95.5(2)
N(1)–Co–N(5)	93.0(1)	N(2)–Co–N(3)	85.2(2)
N(2)–Co–N(4)	94.2(2)	N(2)–Co–N(5)	176.7(1)
N(3)–Co–N(4)	93.0(2)	N(3)–Co–N(5)	91.8(2)
N(4)–Co–N(5)	84.5(2)	Co–S–O(1)	117.0(2)
Co–S–O(2)	118.4(3)	Co–S–C(1)	82.4(2)
Co–N(2)–C(6)	109.9(3)	Co–N(3)–C(7)	109.4(3)
Co–N(4)–C(8)	108.1(3)	Co–N(5)–C(9)	111.2(3)
O(1)–S–O(2)	116.1(4)	O(1)–S–C(1)	106.9(2)
O(2)–S–C(1)	109.5(3)	S–C(1)–N(1)	98.2(3)
S–C(1)–C(2)	138.0(4)	C(1)–N(1)–C(5)	119.7(4)
C(1)–C(2)–C(3)	116.2(6)	C(2)–C(3)–C(4)	121.5(5)
C(3)–C(4)–C(5)	119.7(6)	N(1)–C(1)–C(2)	123.6(5)
N(1)–C(5)–C(4)	119.3(6)	N(2)–C(6)–C(7)	107.4(3)
N(3)–C(7)–C(6)	106.1(4)	N(4)–C(8)–C(9)	107.1(4)
N(5)–C(9)–C(8)	105.3(4)		

nent of the first d–d band generated by the anisotropic interaction of the antibonding π* orbital of the coordinating oxygen with the t_{2g} orbitals on the cobalt center (Scheme 2) [16,17]. Although the π* orbital of the oxygen atom can overlap with the filled dπ orbitals on the cobalt center, the geometry imposed by the chelating nature of the ligand allows only the d_{yz} orbital to overlap with the π* orbital of the oxygen to form significant π back-bonding from the filled Co dπ orbital(s) to the O–S π system. This in turn must split the energetic degeneracy of the two d orbitals (d_{yz} and d_{xz}) in the C_{4v} symmetry, resulting in a splitting of the first d–d band. We estimated the mean energy of the first d–d band for this complex (**4**) to be 20 300 cm^{-1} (493 nm) on the basis of Shimura's treatment [17,18]. Because the pyse-*N*,*S* complex (**2**) shows the first d–d absorption band at 481 nm (20 800 cm^{-1}) [4], the ligand field strength of the pyse-*N*,*O* complex (**4**) is a little weaker than that of **2**. The intense S→Co charge transfer (CT) band at 378 nm (26 500 cm^{-1}) of **2** disappears upon linkage isomerization, and the new band at

Table 5
Final energy terms (kJ mol^{-1}) from the minimization for the complexes **2**, **3**, **4** and **5**

Complex	Total	Bond	Angle	Nonbonded	Torsion
$\Lambda(R)$-[Co(pyse-*N,S*)$(en)_2]^{2+}$ ($\Lambda(R)$-**2**)	135.4	6.4	115.1	4.0	9.8
$\Lambda(S)$-[Co(pyse-*N,S*)$(en)_2]^{2+}$ ($\Lambda(S)$-**2**)	137.5	6.3	116.7	4.3	10.2
[Co(pysi-*N,S*)$(en)_2]^{2+}$ (**3**)	130.0	7.1	108.5	5.4	9.1
[Co(pyse-*N,O*)$(en)_2]^{2+}$ (**4**)	56.7	5.2	29.9	9.4	12.2
$\Lambda(R)$-[Co(pysi-*N,O*)$(en)_2]^{2+}$ ($\Lambda(R)$-**5**)	59.0	6.6	32.3	8.4	11.8
$\Lambda(S)$-[Co(pysi-*N,O*)$(en)_2]^{2+}$ ($\Lambda(S)$-**5**)	58.2	7.1	32.0	7.5	11.6

368 nm (27 200 cm^{-1}) can be assigned to the CT transition from the oxygen of the sulfenate moiety to cobalt.

3.2. Sulfinato complex

Most cobalt(III) complexes containing a sulfinate ligand show Co–S bonding. Treatment of [Co(pyt)$(en)_2]^{2+}$ (**1**) with excess H_2O_2 afforded the orange sulfinato-*N,S* complex, [Co(pysi-*N,S*)$(en)_2]^{2+}$ (**3**); a net 4-equiv oxidation of the coordinating sulfur took place. Complex **3** isomerizes easily to the sulfinato-*N,O* complex, [Co(pysi-*N,O*)$(en)_2]^{2+}$ (**5**, *vide infra*). The X-ray analysis of the oxidation product of [Co(pyt)$(en)_2](ClO_4)_2$ revealed that [Co(pysi-*N,S*)$(en)_2](ClO_4)_2$ (**3**) cocrystallized with [Co(pysi-*N,O*)$(en)_2](ClO_4)_2$ (**5**), and the product will be designated as **3/5**. The determined structure showed a static disorder at the sulfinate site of the chelate ring.

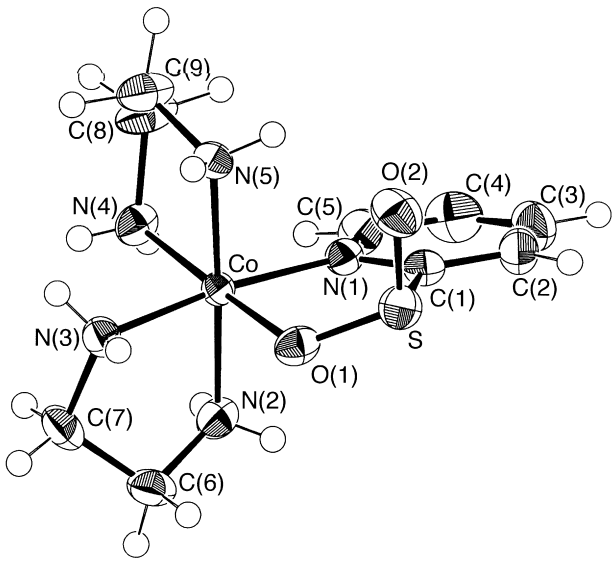

Fig. 4. An ORTEP drawing for the complex cation, $\Lambda(S)$-[Co(pysi-*N,O*)$(en)_2]^{2+}$ ($\Lambda(S)\Delta(R)$-**5**), with thermal ellipsoids at 50% probability.

Table 6
Selected bond lengths [l (Å)] and bond angles [φ (deg)] for $\Lambda(S)\Delta(R)$-$[Co(pysi\text{-}N,O)(en)_2]^{2+}$ ($\Lambda(S)\Delta(R)$-**5**)

Co–O(1)	1.919(2)	Co–N(1)	1.957(3)
Co–N(2)	1.947(3)	Co–N(3)	1.941(3)
Co–N(4)	1.957(3)	Co–N(5)	1.965(3)
S–O(1)	1.513(3)	S–O(2)	1.490(3)
S–C(1)	1.815(4)	N(1)–C(1)	1.354(4)
N(1)–C(5)	1.346(4)	N(2)–C(6)	1.478(5)
N(3)–C(7)	1.482(4)	N(4)–C(8)	1.499(5)
N(5)–C(9)	1.474(5)	C(1)–C(2)	1.373(5)
C(2)–C(3)	1.369(6)	C(3)–C(4)	1.359(6)
C(4)–C(5)	1.376(5)	C(6)–C(7)	1.493(5)
C(8)–C(9)	1.463(5)		
O(1)–Co–N(1)	85.0(1)	O(1)–Co–N(2)	87.6(1)
O(1)–Co–N(3)	88.3(1)	O(1)–Co–N(4)	177.1(1)
O(1)–Co–N(5)	92.2(1)	N(1)–Co–N(2)	90.5(1)
N(1)–Co–N(3)	172.1(1)	N(1)–Co–N(4)	95.5(1)
N(1)–Co–N(5)	92.4(1)	N(2)–Co–N(3)	85.0(1)
N(2)–Co–N(4)	95.3(2)	N(2)–Co–N(5)	177.1(1)
N(3)–Co–N(4)	91.4(2)	N(3)–Co–N(5)	92.1(1)
N(4)–Co–N(5)	84.9(1)	Co–O(1)–S	120.2(1)
Co–N(1)–C(1)	115.0(2)	Co–N(1)–C(5)	127.7(2)
Co–N(2)–C(6)	110.1(2)	Co–N(3)–C(7)	109.9(2)
Co–N(4)–C(8)	108.7(2)	Co–N(5)–C(9)	110.8(2)
O(1)–S–O(2)	110.6(1)	O(1)–S–C(1)	96.0(1)
O(2)–S–C(1)	103.6(2)	S–C(1)–N(1)	116.1(2)
S–C(1)–C(2)	121.2(3)	C(1)–N(1)–C(5)	117.1(3)
C(1)–C(2)–C(3)	119.1(4)	C(2)–C(3)–C(4)	118.8(4)
C(3)–C(4)–C(5)	120.2(4)	N(1)–C(1)–C(2)	122.8(3)
N(1)–C(5)–C(4)	121.9(4)	N(2)–C(6)–C(7)	106.3(3)
N(3)–C(7)–C(6)	106.6(3)	N(4)–C(8)–C(9)	107.7(3)
N(5)–C(9)–C(8)	108.9(3)		

The sulfinate moiety for the *S*-bonded complex (**3**) consists of the atoms Co–SO(1)O(2)–C(1) (Fig. 3), while the moiety for the *O*-bonded one (**5**) consists of Co–O(1)′–S′O(2)′–C(1) [primed atoms denote the disordered ones (**5**) in **3/5**]. Fig. 3 shows an ORTEP drawing of $[Co(pysi\text{-}N,S)(en)_2]^{2+}$ (**3**). The bond lengths and angles of **3** are listed in Table 4. The pysi ligand coordinates to cobalt with the nitrogen and sulfur and forms a four-membered chelate ring. The *S*-bonded sulfinate ligand exerts a small trans influence (0.020(5) Å). This lengthening is only marginally smaller than that found in the analogous thiolate complex (0.023(6) Å) [4].

The pysi-*N*,*S* complex (**3**) was unstable and easily converted photochemically or thermally to the linkage-isomerized pysi-*N*,*O* complex (**5**, Scheme 1), and the first-order rate constant in water was $5.6 \times 10^{-5}\ s^{-1}$ at 30 °C in the dark. Adamson and co-workers prepared the sulfinato-*O* cobalt(III) complex, $[Co\{OS(O)CH_2CH_2NH_2\text{-}N,O\}(en)_2]^{2+}$, for the first time upon irradiation of the sulfinato-*S* complex, $[Co\{S(O)_2CH_2CH_2NH_2\text{-}N,S\}(en)_2]^{2+}$ [1]. $[Co\{OS(O)CH_2\text{-}CH_2NH_2\text{-}N,O\}(en)_2]^{2+}$ reverts thermally to the starting *N*,*S*-chelate complex. On

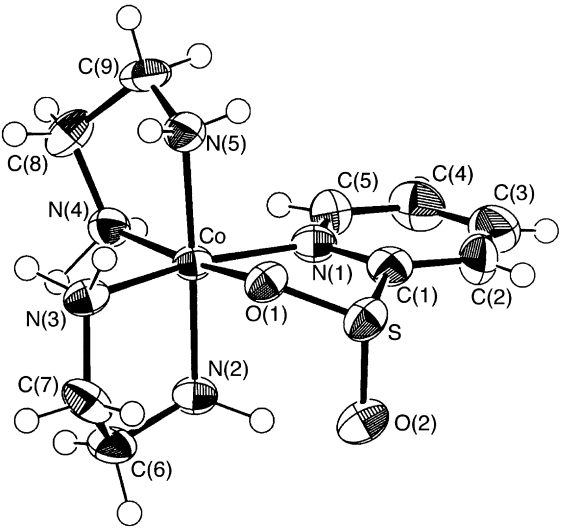

Fig. 5. An ORTEP drawing for the complex cation, $\Lambda(R)$-$[Co(pysi\text{-}N,O)(en)_2]^{2+}$ ($\Lambda(R)$-**5**), with thermal ellipsoids at 50% probability.

the other hand, the pysi-*N*,*O* complex is thermodynamically stable and does not isomerize to the pysi-*N*,*S* complex. The difference in stability for a thermal back-reaction between $[Co\{OS(O)CH_2CH_2NH_2\text{-}N,O\}(en)_2]^{2+}$ and the pysi-*N*,*O* complex may be explained by considering the difference in the intramolecular strain between the *S*-bonded and *O*-bonded isomers. Molecular mechanics calculations revealed that the strain energy of the four-membered pysi-*N*,*S* chelate (**3**) is much larger than that of the five-membered pysi-*N*,*O* chelate (**5**) (Table 5). This result is in accord with our observation of complete conversion to the pysi-*N*,*O* complex upon thermal or photo-assisted equilibrium. Probably, $[Co\{OS(O)CH_2CH_2NH_2\text{-}N,O\}(en)_2]^{2+}$ having a six-membered chelate ring involves more strain than $[Co\{S(O)_2CH_2CH_2NH_2\text{-}N,S\}(en)_2]^{2+}$. A similar difference in thermal stability between the four-membered and five-membered chelate rings was observed between the pyse-*N*,*S* and pyse-*N*,*O* complexes. The thermal stability of the five-membered pyse-*N*,*O* complex is also in accord with the results of the calculations (Table 5).

Upon linkage isomerization from sulfinato-*S* to sulfinato-*O*, the sulfur atom becomes chiral (*R* and *S*), and because there is another chiral center around the cobalt atom (Δ and Λ), two kinds of racemic salt, $\Lambda(R)\Delta(S)$ and $\Lambda(S)\Delta(R)$, are possible. The crude product was revealed to be an almost equimolar mixture of the two types on the basis of the ^1H NMR spectrum. Fractional crystallization of the perchlorate salt of racemic **5** twice from water gave essentially pure $\Lambda(S)\Delta(R)$ as the less soluble part, and a piece of the crystal was used for the X-ray structure determination. An ORTEP drawing of $\Lambda(S)$-$[Co(pysi\text{-}N,O)(en)_2]^{2+}$ [the enantiomer, $\Delta(R)$, is also involved in the unit cell] is shown in Fig. 4. The bond lengths and angles are listed in Table 6. The pysi ligand coordinates to cobalt with the nitrogen

Table 7
Selected bond lengths [l (Å)] and bond angles [φ (deg)] for $\Lambda(R)$-[Co(pysi-N,O)$(en)_2]^{2+}$ ($\Lambda(R)$-**5**)

Co–O(1)	1.916(5)	Co–N(1)	1.976(7)
Co–N(2)	1.963(7)	Co–N(3)	1.936(7)
Co–N(4)	1.954(8)	Co–N(5)	1.941(8)
S–O(1)	1.537(5)	S–O(2)	1.497(6)
S–C(1)	1.805(9)	N(1)–C(1)	1.34(1)
N(1)–C(5)	1.35(1)	N(2)–C(6)	1.46(1)
N(3)–C(7)	1.48(1)	N(4)–C(8)	1.49(1)
N(5)–C(9)	1.47(1)	C(1)–C(2)	1.35(1)
C(2)–C(3)	1.35(1)	C(3)–C(4)	1.39(1)
C(4)–C(5)	1.36(1)	C(6)–C(7)	1.50(1)
C(8)–C(9)	1.49(1)		
O(1)–Co–N(1)	84.6(3)	O(1)–Co–N(2)	94.4(3)
O(1)–Co–N(3)	85.9(3)	O(1)–Co–N(4)	171.4(3)
O(1)–Co–N(5)	87.3(3)	N(1)–Co–N(2)	89.6(3)
N(1)–Co–N(3)	169.1(3)	N(1)–Co–N(4)	99.5(3)
N(1)–Co–N(5)	92.4(3)	N(2)–Co–N(3)	85.7(3)
N(2)–Co–N(4)	93.1(3)	N(2)–Co–N(5)	177.5(3)
N(3)–Co–N(4)	90.6(3)	N(3)–Co–N(5)	92.7(3)
N(4)–Co–N(5)	85.0(3)	Co–O(1)–S	118.4(3)
Co–N(1)–C(1)	116.7(6)	Co–N(1)–C(5)	128.6(6)
Co–N(2)–C(6)	110.5(6)	Co–N(3)–C(7)	108.4(5)
Co–N(4)–C(8)	109.3(5)	Co–N(5)–C(9)	110.7(6)
O(1)–S–O(2)	109.8(3)	O(1)–S–C(1)	97.4(4)
O(2)–S–C(1)	100.8(3)	S–C(1)–N(1)	114.2(7)
S–C(1)–C(2)	121.1(8)	C(1)–N(1)–C(5)	114.7(8)
C(1)–C(2)–C(3)	120(1)	C(2)–C(3)–C(4)	118(1)
C(3)–C(4)–C(5)	118(1)	N(1)–C(1)–C(2)	124.4(9)
N(1)–C(5)–C(4)	124.8(9)	N(2)–C(6)–C(7)	107.1(7)
N(3)–C(7)–C(6)	107.7(7)	N(4)–C(8)–C(9)	107.2(7)
N(5)–C(9)–C(8)	106.3(7)		

and oxygen instead of the nitrogen and sulfur as in the *S*-bonded one, and the number of chelate ring members increases from four to five. The two diastereomers of Λ-[Co(pysi-N,O)$(en)_2]^{2+}$ were separated by SP-Sephadex column chromatography. Fig. 5 shows a perspective view of the $\Lambda(R)$-[Co(pysi-N,O)$(en)_2]^{2+}$ cation which was obtained from the eluate containing the faster eluted portion of the band (eluent: 0.15 M $Na_2[Sb_2\{(+)\text{-tart}\}_2]$). The bond lengths and angles are listed in Table 7. The sulfinate oxygen in either of the two complexes does not induce a significant trans influence. Kinetic studies of reversible isomerization (epimerization) between the two isomers of Λ-[Co(pysi-N,O)$(en)_2]^{2+}$ were performed in aqueous solutions at 60 °C by observing the change in the CD strengths at 325 nm. No significant change in the UV–vis spectrum was observed during the epimerization.

The forward and reverse first-order rate constants, $k_{\Lambda(R)\rightarrow\Lambda(S)}$ and $k_{\Lambda(S)\rightarrow\Lambda(R)}$, were obtained from k_{obs} ($k_{obs}=k_{\Lambda(R)\rightarrow\Lambda(S)}+k_{\Lambda(S)\rightarrow\Lambda(R)}$) and the equilibrium constant K_{eq} ($K_{eq}=k_{\Lambda(R)\rightarrow\Lambda(S)}/k_{\Lambda(S)\rightarrow\Lambda(R)}=[\Lambda(S)]_{eq}/[\Lambda(R)]_{eq}$). The rate constants were $k_{obs}=7.2\times10^{-6}\,s^{-1}$, $k_{\Lambda(R)\rightarrow\Lambda(S)}=5.5\times10^{-6}\,s^{-1}$ and $k_{\Lambda(S)\rightarrow\Lambda(R)}=1.7\times10^{-6}\,s^{-1}$, and

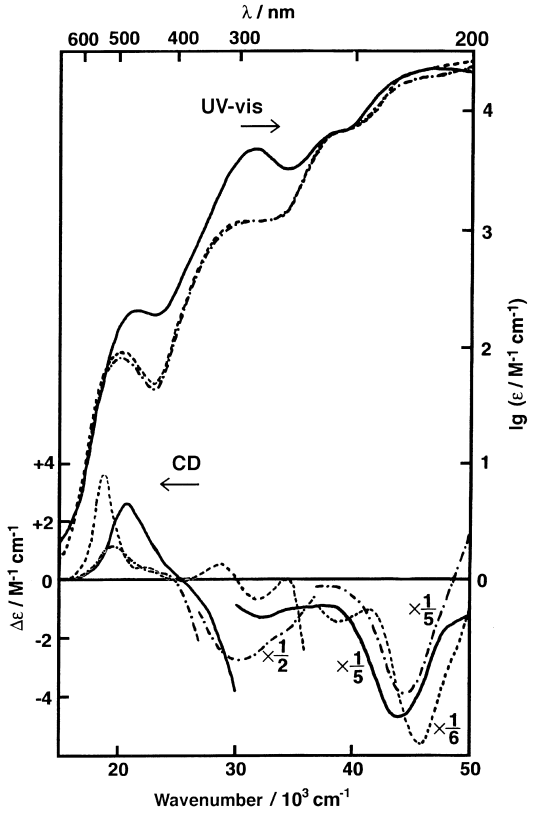

Fig. 6. UV–vis and CD spectra of the two diastereomers of Λ-[Co(pysi-*N*,*O*)(en)$_2$](ClO$_4$)$_2$ (Λ-**5**): Λ(*R*)-isomer (– · –), Λ(*S*)-isomer (· · ·) and Λ-[Co(pysi-*N*,*S*)(en)$_2$](ClO$_4$)$_2$ (Λ-**3**) (———).

the equilibrium constant (K_{eq}) was 3.2. Molecular mechanics calculations also revealed that the Λ(*S*)-isomer is more stable than the Λ(*R*)-isomer, although the energy difference (0.8 kJ mol^{-1}, Table 5) is smaller than that (3.2 kJ mol^{-1}) calculated on the basis of the equilibrium constant.

Fig. 6 compares the UV–vis spectra of Λ(*R*)- and Λ(*S*)-[Co(pysi-*N*,*O*)(en)$_2$]$^{2+}$ with that of Λ-[Co(pysi-*N*,*S*)(en)$_2$]$^{2+}$. The pysi-*N*,*O* complexes have a much weaker ligand field strength than does the pysi-*N*,*S* one; the latter shows the first d–d absorption band at 458 nm (21 800 cm^{-1}), while those of the former complexes appear at 494 nm (20 200 cm^{-1}). A similar difference in the UV–vis spectra has been reported between the sulfinato-*S* and the corresponding sulfinato-*O* complexes such as [Co{S(O)$_2$CH$_2$CH$_2$NH$_2$-*N*,*S*}(en)$_2$]$^{2+}$ (432 nm, 23 100 cm^{-1}) and its photoproduct, [Co{OS(O)CH$_2$CH$_2$NH$_2$-*N*,*O*}(en)$_2$]$^{2+}$ (512 nm, 19 500 cm^{-1}) [1]. The intense S→Co charge transfer (CT) band at 317 nm (31 500 cm^{-1}) of the pysi-*N*,*S* complex disappears upon linkage isomerization, and the new band at 340 nm (29 400 cm^{-1}) can be assigned to the CT transition from the oxygen of the sulfinate moiety to cobalt. The CD spectra of Λ(*R*)- and Λ(*S*)-[Co(pysi-*N*,*O*)(en)$_2$]$^{2+}$ are also shown in

Fig. 6. The CD contribution due to the chiral sulfur atom was estimated assuming the additivity rule [19,20]. The (*R*)-sulfur atom has a negative vicinal CD contribution in the first d–d band region, which is opposite to that obtained from Λ(*R*)- and Λ(*S*)-[Co{OS(O)$CH_2CH_2NH_2$-*N*,*O*}$(en)_2$]$^{2+}$ [21]. The apparent discrepancy may be related to the difference in chelate ring members which would cause the difference in the intramolecular strain.

3.3. Sulfonato complex

Although a sulfonate ion can coordinate to a metal ion through the oxygen atom, its affinity to cobalt(III) is usually low. For example, [Co{$OS(O)_2CH_3$}$(NH_3)_5$]$^{2+}$ is easily aquated ($t_{1/2}$ ca. 58 min, at 25 °C) [22]. We expected that 2-pyridinesulfonate ion might coordinate to cobalt(III) with the nitrogen and oxygen atoms to form a stable five-membered chelate ring. The [Co(pyso-*N*,*O*)$(en)_2$]$^{2+}$ (**6**) complex was prepared by the reaction of *cis*-[Co{$OS(O)_2CF_3$}$_2(en)_2$]$^+$ with the 2-pyridinesulfonate ligand or by the oxidation of [Co(pyse-*N*,*O*)$(en)_2$]$^{2+}$ (**4**) with H_2O_2. An ORTEP drawing of [Co(pyso-*N*,*O*)$(en)_2$]$^{2+}$ (**6**) is shown in Fig. 7. Bond lengths and angles are listed in Table 8. The 2-pyridinesulfonate ligand coordinates to cobalt with the nitrogen and oxygen atoms. The bond length of S–O(1) (1.503(3) Å) is greater than S–O(2) (1.445(3) Å) and S–O(3) (1.458(3) Å).

As the formal oxidation state of the sulfur increases along the sulfenato-*O*–sulfinato-*O*–sulfonato-*O* series (0, +II, +IV), the cobalt to coordinating oxygen bond length increases (1.893(3) Å, 1.916(5) Å, 1.956(2) Å). The short Co–O bond in the pyse-*O* chelate may be related to the delocalization of the molecular orbitals which facilitates π back-bonding from the cobalt to the coordinating oxygen

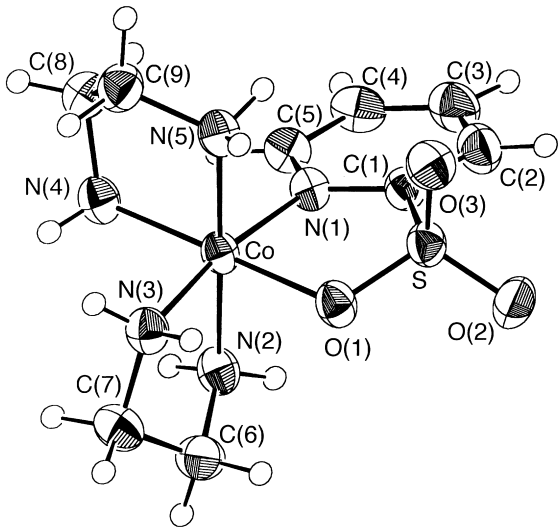

Fig. 7. An ORTEP drawing for the complex cation, [Co(pyso-*N*,*O*)$(en)_2$]$^{2+}$ (**6**), with thermal ellipsoids at 50% probability.

Table 8
Selected bond lengths [l (Å)] and bond angles [φ (deg)] for $[Co(pyso\text{-}N,O)(en)_2]^{2+}$ (**6**)

Co–O(1)	1.956(2)	Co–N(1)	1.983(3)
Co–N(2)	1.964(3)	Co–N(3)	1.974(3)
Co–N(4)	1.968(3)	Co–N(5)	1.983(3)
S–O(1)	1.503(3)	S–O(2)	1.445(3)
S–O(3)	1.458(3)	S–C(1)	1.796(3)
N(1)–C(1)	1.363(5)	N(1)–C(5)	1.365(4)
N(2)–C(6)	1.497(5)	N(3)–C(7)	1.507(6)
N(4)–C(8)	1.505(6)	N(5)–C(9)	1.493(5)
C(1)–C(2)	1.389(6)	C(2)–C(3)	1.403(6)
C(3)–C(4)	1.386(6)	C(4)–C(5)	1.395(6)
C(6)–C(7)	1.512(6)	C(8)–C(9)	1.532(6)
O(1)–Co–N(1)	85.6(1)	O(1)–Co–N(2)	87.2(1)
O(1)–Co–N(3)	85.9(1)	O(1)–Co–N(4)	177.1(1)
O(1)–Co–N(5)	93.5(1)	N(1)–Co–N(2)	90.6(1)
N(1)–Co–N(3)	170.7(1)	N(1)–Co–N(4)	96.6(1)
N(1)–Co–N(5)	90.4(1)	N(2)–Co–N(3)	85.2(1)
N(2)–Co–N(4)	94.6(1)	N(2)–Co–N(5)	178.9(2)
N(3)–Co–N(4)	92.1(1)	N(3)–Co–N(5)	93.9(1)
N(4)–Co–N(5)	84.6(1)	Co–O(1)–S	116.0(1)
Co–N(1)–C(1)	115.2(2)	Co–N(1)–C(5)	127.1(3)
Co–N(2)–C(6)	109.3(2)	Co–N(3)–C(7)	109.9(2)
Co–N(4)–C(8)	110.7(2)	Co–N(5)–C(9)	110.4(2)
O(1)–S–O(2)	112.5(2)	O(1)–S–O(3)	111.8(2)
O(2)–S–O(3)	114.8(2)	O(1)–S–C(1)	100.6(2)
O(2)–S–C(1)	109.3(2)	O(3)–S–C(1)	106.7(2)
S–C(1)–N(1)	114.0(3)	S–C(1)–C(2)	122.1(3)
C(1)–N(1)–C(5)	117.6(3)	C(1)–C(2)–C(3)	117.4(4)
C(2)–C(3)–C(4)	119.6(4)	C(3)–C(4)–C(5)	119.8(3)
N(1)–C(1)–C(2)	123.9(3)	N(1)–C(5)–C(4)	121.6(3)
N(2)–C(6)–C(7)	105.5(3)	N(3)–C(7)–C(6)	107.5(4)
N(4)–C(8)–C(9)	106.5(3)	N(5)–C(9)–C(8)	105.5(3)

(Scheme 2). The higher planarity of the pyse-*O* chelate over the pysi-*O* chelate [23] will also help the π back-bonding. In the case of the sulfonate ligand, no effective π back-bonding interaction will be expected between the ligating oxygen and the Co dπ orbitals, because all the sulfur valence orbitals are used for bonding with the neighboring atoms and there is no π bonding between the sulfur and the ligating oxygen. Thus, the long Co–O bond in the pyso complex will be related to the absence of the π interaction. The bond of S to pyridine-C in the pyse-*N*,*O* complex (1.733(5) Å) is shorter than those of the pysi-*N*,*O* complex (1.805(9) Å) and the pyso-*N*,*O* complex (1.796(3) Å); this is also explained in terms of the delocalized MO of the pyse-*O* chelate ring.

We carried out electrochemical measurements of the *N*,*O*-chelate complexes (**4**, **5** and **6**), because the method gives information on the effects of the ligand on the cobalt center. All complexes in water showed irreversible redox behavior in CV, and thus the reduction potentials were obtained by RDE measurements, $|E_{1/4} - E_{3/4}|$

values being 80–130 mV. As the oxidation state of the sulfur increases, the reduction potentials changed to the less negative side (−0.41 V, −0.31 V, −0.04 V), which means the Co(III) center became easier to reduce and the energy levels of the dσ* orbital became lower. This results from less interaction between Co and the ligands. Less interaction implies that the σ interaction of the cobalt to the coordinating oxygen atom also decreases with the oxidation state of the sulfur atom. Thus, the electrochemical data are consistent with the order of the Co–O bond length of the three cobalt(III) complexes obtained by the X-ray method.

Sulfur oxidation causes a down-field shift of the ^{1}H NMR resonances of the pyridine protons (7.24–8.11 ppm, 7.89–8.63 ppm, 8.05–8.64 ppm). This is explained in terms of increasing electron withdrawal from the pyridine hydrogen orbitals with the increasing electronegativity of the substituent.

The pyso complex (**6**) shows the first d–d absorption band at 20 600 cm^{-1} (486 nm, Fig. 8Table 3). The pyso ligand has the strongest ligand field strength among the ligands studied here. The shoulder at 37 500 cm^{-1} (267 nm) may be assigned to the CT transition from the sulfonate oxygen atom to cobalt. The pyso complex could be resolved by SP-Sephadex column chromatography, 0.1M $Na_2[Sb_2\{(+)\text{-tart}\}_2]$ being used as the eluent. The $(+)^{CD}_{539}$-isomer, which was eluted faster in column chromatography, can be assigned to the Λ-isomer on the basis of the CD spectral pattern in the first d–d band region [21]. The complex is stable, and no detectable change in the absorption and CD spectra was observed for 20 h

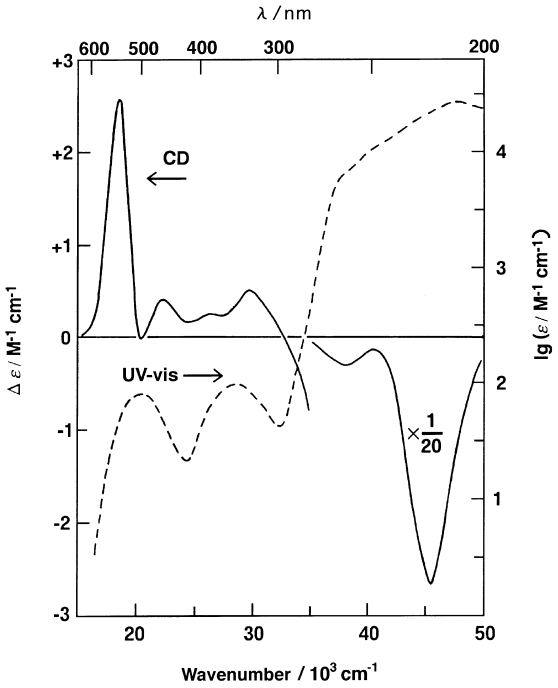

Fig. 8. UV–vis (– – –) and CD (———) spectra of Λ-[Co(pyso-*N*,*O*)(en)$_2$](ClO$_4$)$_2$ (Λ-**6**).

at 50 °C. Ford and Nolan [24] reported that the base hydrolysis products of *cis*-$[CoCl\{NH_2(CH_2)_nSO_3\text{-}N\}(en)_2]^+$ ($n=1$, 2), where the sulfonate groups do not coordinate to Co, were the corresponding hydroxo complexes, and in neither case was the chelated aminoalkanesulfonato complex observed. Thus, they concluded that the sulfonate groups were ineffective in competing with water for the vacant coordination site in the five-coordinate conjugate base intermediate, $[Co\{NH(CH_2)_nSO_3\text{-}N\}(en)_2]^+$ [24]. As far as we know, the present pyso complex is the most stable sulfonatocobalt(III) complex in water [5].

Acknowledgements

This work was supported by Grants-in-Aid for Scientific Research Nos. 05403009 and 07640753 from the Ministry of Education, Science, Sports and Culture. This work was also supported by the Joint Studies Program (1994–1995) of the Institute for Molecular Science.

References

[1] H. Mäcke, V.H. Houlding, A.W. Adamson, J. Am. Chem. Soc. 102 (1980) 6888.
[2] I.K. Adzamli, K. Libson, J.D. Lydon, R.C. Elder, E. Deutsch, Inorg. Chem. 18 (1979) 303.
[3] B.A. Lange, K. Libson, E. Deutsch, R.C. Elder, Inorg. Chem. 15 (1976) 2985.
[4] M. Kita, K. Yamanari, Y. Shimura, Bull. Chem. Soc. Jpn. 62 (1989) 3081.
[5] M. Murata, M. Kojima, M. Kita, S. Kashino, Y. Yoshikawa, Chem. Lett. (1996) 675.
[6] R.F. Evans, H.C. Brown, J. Org. Chem. 27 (1962) 1329.
[7] W. Walter, J. Voß, J. Curts, Justus Liebigs Ann. Chem. 695 (1966) 77.
[8] N.E. Dixon, W.G. Jackson, G.A. Lawrance, A.M. Sargeson, Inorg. Synth. 22 (1983) 103.
[9] C.J. Gilmore, MITHRIL, Program for the Automatic Solution of Crystal Structures from X-ray data, Department of Chemistry, University of Glasgow, Scotland, 1984, excluding **6**. For **6**, G.M. Sheldrick, SHELXS-86, Program for Crystal Structure Determination, University of Göttingen, Germany, 1986.
[10] TEXSAN. Single Crystal Structure Analysis Software, Version 5.0, Molecular Structure Corporation, The Woodlands, TX, 1989.
[11] S.R. Hall, H.D. Flack, J.M. Stewart, Xtal3.2, Program for X-ray Crystal Structure Analysis, Universities of Western Australia, Geneva and Maryland, 1992.
[12] ZINDO and EHMO (CAChe version 3.8), CAChe Scientific, 1995. The calculations were carried out on a Power Macintosh 9500 (Apple) at the Information Processing Center of the Naruto University of Education.
[13] Y. Yoshikawa, J. Comput. Chem. 11 (1990) 326.
[14] N.L. Allinger, Y.H. Yuh, QCPE 12 (1980) 395.
[15] G.R. Brubaker, D.W. Johnson, Coord. Chem. Rev. 53 (1984) 1, and references cited in Ref. [13].
[16] V.H. Houlding, H. Mäcke, A.W. Adamson, Inorg. Chem. 20 (1981) 4279.
[17] Y. Shimura, Bull. Chem. Soc. Jpn. 61 (1988) 693.
[18] Assuming that the d values (in 10^3 cm^{-1}) for en and the pyridine moiety of pyse to be 21.4 and 22.2, respectively [17], three components of the first d–d absorption band of $[Co(pyse\text{-}N,O)(en)_2]^{2+}$ are

expected to appear at

$$\sigma_{N_4} = (21.4 \times 3 + 22.2)/4 = 21.6$$

$$\sigma_{N_3O_{\parallel}} = (21.4 \times 2 + 22.2 + d_{O_{\parallel}})/4$$

$$\sigma_{N_3O_{\perp}} = (21.4 \times 3 + d_{O_{\perp}})/4$$

The observed lower energy band (16 400 cm^{-1}) is attributable to the $\sigma_{N_3O_{\parallel}}$ component, while the higher energy one (22 200 cm^{-1}) to the average of the σ_{N_4} and $\sigma_{N_3O_{\perp}}$ components. Thus, we obtain $d_{O_{\parallel}} = 0.6$, $d_{O_{\perp}} = 27.0$ and $d_{O(pyse)} = (d_{O_{\parallel}} + d_{O_{\perp}})/2 = 13.8$. The mean energy of the first d–d band for $[Co(pyse\text{-}N,O)(en)_2]^{2+}$ is estimated to be $(21.4 \times 4 + 22.2 + 13.8)/6 = 20.3$ ($\times 10^3$ cm^{-1}).

[19] B.E. Douglas, S. Yamada, Inorg. Chem. 4 (1965) 1561.
[20] B.E. Douglas, Inorg. Chem. 4 (1965) 1813.
[21] K. Yamanari, Y. Shimura, Chem. Lett. (1984) 761.
[22] W.G. Jackson, S.S. Jurisson, M.A. O'Leary, Inorg. Chem. 32 (1993) 445.
[23] All complexes in the series, pyse-*N*,*O* (**4**), pysi-*N*,*O* (**5**) and pyso-*N*,*O* (**6**), show fundamentally similar structures, comprised of the chelate system with a pyridine ring. The chelate $\overline{Co–O–S–C–N}$ portion of the ligand takes an envelope conformation, and the oxygen is deviated from the least-squares plane (0.49 Å for **4**, 0.44 Å for **5** and 0.47 Å for **6**). Deviation from planality as defined by the angle between the least-squares planes of CoSCN and the pyridine ring is 0.73° for **4**, 3.15° for **5**, and 0.97° for **6**.
[24] P.D. Ford, K.B. Nolan, Inorg. Chim. Acta 43 (1980) 83.